

Remote Monitoring of Subsurface Flow Conditions in Rivers

Christopher J. Zappa

Lamont-Doherty Earth Observatory of Columbia University

Ocean and Climate Physics Division

61 Route 9W

Palisades, NY 10964

Phone: (845) 365-8547 fax: (845) 365-8157 email: zappa@ldeo.columbia.edu

Award Number : N00014-11-1-0922

LONG-TERM GOALS

The primary research goal is to develop techniques to determine subsurface turbulence from remote measurements using infrared imaging of the skin layer. We aim to infer flow rate, turbulence intensity and subsurface-generated turbulent structures from surface temperature patterns. We will take advantage of the two complementary indicators of subsurface flow provided by IR imagery: the thermal structures measured directly and the surface velocity fields obtained through various image processing techniques. We will (1) analyze the variability and structures of the thermal boundary layer, (2) compute the surface flow field from the IR imagery and infer further surface turbulence characteristics, (3) determine to which extent the turbulence in the boundary layer is due to surface forcing by analysis of the air-sea flux data and (4) determine empirical relationships of subsurface flow characteristics and of turbulence derived from in situ sub-surface data to the observed turbulence in the IR imagery. We further aim to determine the limits of remotely inferring flow rates, subsurface turbulence and bed stress from IR imagery. We will investigate how different wind, tides and wave breaking conditions affect our ability to remotely measure subsurface flow characteristics.

OBJECTIVES

The skin temperature is governed by surface and subsurface processes. Net air-water heat flux leads to a cooler thermal boundary layer (TBL) compared to the underlying bulk layer. Turbulent motions resulting from wind forcing at the air-sea interface and from turbulent eddies generated within the water column, disrupt the TBL, mixing it with the bulk layer. During the last century links between air-water transfer and bulk turbulence were researched (*Brumley and Jirka, 1988; Danckwerts, 1951*). Only in the last decade, has the TBL been recognized as the intermediate step between subsurface turbulence and air-water transfer and as such was used as a more direct indicator for air-water transfer (*McKenna and McGillis, 2004*). This study will use the TBL as a direct indicator for subsurface turbulence and provide predictive relationships of the surface-bulk connection. It will result in a be a set of universal curves connecting remotely collected surface measurements to fundamental local flow quantities – the flow depth, the bed stress, the bulk mean flow and the bulk turbulent kinetic energy.

Report Documentation Page			Form Approved OMB No. 0704-0188		
<p>Public reporting burden for the collection of information is estimated to average 1 hour per response, including the time for reviewing instructions, searching existing data sources, gathering and maintaining the data needed, and completing and reviewing the collection of information. Send comments regarding this burden estimate or any other aspect of this collection of information, including suggestions for reducing this burden, to Washington Headquarters Services, Directorate for Information Operations and Reports, 1215 Jefferson Davis Highway, Suite 1204, Arlington VA 22202-4302. Respondents should be aware that notwithstanding any other provision of law, no person shall be subject to a penalty for failing to comply with a collection of information if it does not display a currently valid OMB control number.</p>					
1. REPORT DATE 30 SEP 2013	2. REPORT TYPE	3. DATES COVERED 00-00-2013 to 00-00-2013			
4. TITLE AND SUBTITLE Remote Monitoring of Subsurface Flow Conditions in Rivers			5a. CONTRACT NUMBER		
			5b. GRANT NUMBER		
			5c. PROGRAM ELEMENT NUMBER		
6. AUTHOR(S)			5d. PROJECT NUMBER		
			5e. TASK NUMBER		
			5f. WORK UNIT NUMBER		
7. PERFORMING ORGANIZATION NAME(S) AND ADDRESS(ES) Lamont-Doherty Earth Observatory of Columbia University,Ocean and Climate Physics Division,61 Route 9W,Palisades,NY,10964			8. PERFORMING ORGANIZATION REPORT NUMBER		
9. SPONSORING/MONITORING AGENCY NAME(S) AND ADDRESS(ES)			10. SPONSOR/MONITOR'S ACRONYM(S)		
			11. SPONSOR/MONITOR'S REPORT NUMBER(S)		
12. DISTRIBUTION/AVAILABILITY STATEMENT Approved for public release; distribution unlimited					
13. SUPPLEMENTARY NOTES					
14. ABSTRACT					
15. SUBJECT TERMS					
16. SECURITY CLASSIFICATION OF: a. REPORT b. ABSTRACT c. THIS PAGE unclassified unclassified unclassified			17. LIMITATION OF ABSTRACT Same as Report (SAR)	18. NUMBER OF PAGES 7	19a. NAME OF RESPONSIBLE PERSON

APPROACH

Building on our extensive expertise in IR imagery and our experience in making near-boundary turbulence measurements, we aim to determine empirical relationships between surface length-scales and flow and sub-surface flow and turbulence. During the prototype field campaign, data was collected with the following instruments:

- IR camera: a Cedip Jade III longwave camera was mounted a pan/tilt system from the A-frame of a moored ship. This set up allowed us to move the camera with the current so to always view upstream of the ship. The Cedip Jade III offers better than 15 mK temperature resolution, with 200 Hz max frame rate, 14-bit digitization, and 320 x 240 pixels. The sampling frequency was set to 60 Hz.
- Air-Sea Flux package: a meteorological station was mounted on a piling neighbouring the ship to get measurements of wind speed & direction, relatively humidity, atmospheric pressure, air temperature, solar insolation, and longwave radiation.
- Acoustic Doppler Velocimeter (ADV): a Nortek Vector type ADV was mounted on the aforementioned piling at 11m above the River bed. Data was collected in 10 min bursts at top of every $\frac{1}{2}$ hr, with a sampling frequency 32Hz.
- Higher Resolution Profilers: 2 Nortek Aquadopp were mounted on the piling at 3 and 6 m above the river bed. They offer a 1-cm resolution. Data was collected in 59.9 min burst at top of every hour, with a sampling frequency 2 Hz.
- CTDs: 3 CTDs were mounted on the piling at the same levels as the ADV and Aquadopps

The team's envisaged data analysis effort includes: image processing and analysis of the IR imagery to characterize surface turbulence. This comprises calculation of the statistical moments, histograms to assess surface skin temperature variability, and determination of length scales of the skin temperature structures. Further 3 methods to determine the surface velocity field from the IR imagery will allow inferring integral length scales, as well as the surface turbulent kinetic energy and calculation of divergence. The bulk Reynolds number can then be determined from the divergence. Analysis of the Aquadopps, ADV and CTD data combined will provide a robust measure of subsurface turbulent, convective, and advective motions. Links between the subsurface and surface turbulence will be investigated, keeping in mind that the observed turbulence at the surface is partly due to surface forcing. Processing and analysis of the direct measurement of heat, mass and momentum fluxes across the air-water interface along with measurements of the radiative forcing will permit to separate the different processes (wind-driven, bed-driven, buoyancy-driven, and convective) which lead to surface turbulence.

WORK COMPLETED

Our efforts FY12 comprised image processing and analysis of IR imagery taken from the ship and analysis of in situ measurements so to address point (3) and (4) of the long term goals. Skin temperature variance was shown to decrease with increasing wind speed and latent heat flux. Surface integral length scales were determined from the skin temperature and are shown to be linearly related to water column depth. Surface currents were derived via three algorithms: Digital Particle Image Velocimetry, Optical Flow and Spectral Advection Surface. They gave estimates that were highly correlated to the

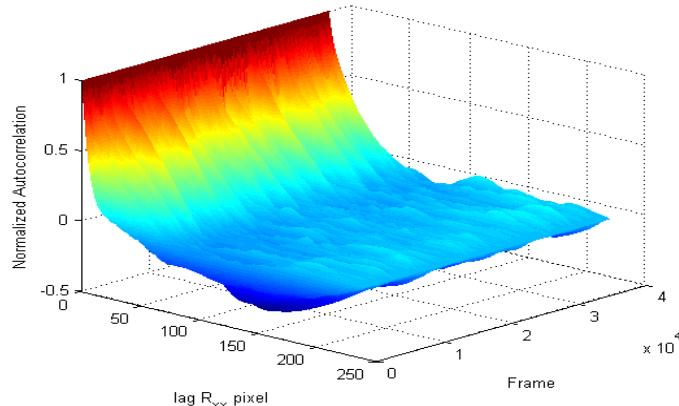
subsurface flow measurements with comparable 10 minute mean magnitudes. We have presented our results at the AGU Fall Meeting, San Francisco, CA, USA in December 2012.

RESULTS

Characteristic surface length scales

In order to determine the characteristic surface length scale we computed a normalized auto-covariance function for each row and column of each frame (an example of which is shown in Figure 1). Then a frame mean normalized auto-covariance function was computed by averaging these over rows and columns. The characteristic integral length scale was determined as the distance at which the temperatures are no longer correlated, i.e. corresponding to the smallest lag at which the frame mean auto-covariance function is equal to zero. Figure 1 shows scatter plots of the integral length scales derived from the skin temperature fields versus water depth. It suggests the scale of the surface features (δ) is strongly linearly correlated ($r^2=0.86$) to the water depth (D), with a slope of $D/\delta \sim 9.5$.

(a)



(b)

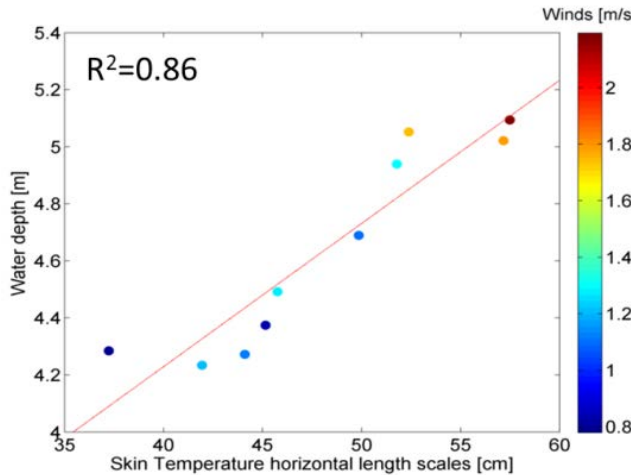


Figure 1 - (a) Sample timeseries of the frame averaged normalized spatial autocorrelation of the thermal imagery for various lags. (b) Scatter plot of the surface scales derived from the spatial autocorrelation functions against height of the water column

The first hypothesis that comes to mind as to the physical explanation of the relation between surface scales and depth, is that the size of the boils that come up to the surface disrupting the TBL, increases with the water column depth. This hypothesis is supported by the work of Korchokha [1968] and Jackson [1978] who found that the size of boils coming up to the surface is proportional to the water column depth. Jackson [1978] plotted the boil diameter (\mathcal{O}) against the water depth (d) measured by Korchokha [1968] in the Polomet River in Russia and showed that they correlate well within a band delimited by the two lines: $d/\mathcal{O}=1.75$ and $d/\mathcal{O}=3.7$. These slopes are much smaller than the one we observed in this study. This could maybe be explained by the different origin of the signal observed. Here, the temperature signal is detected, whereas Jackson [1978] used visual observations for his estimates. The relation between boil diameter and flow depth may be expected from the scaling relation proposed by Rao et al. [1971], relating the boundary layer thickness (δ) to the free stream velocity (U_∞) and a mean periodicity of bursting: $U_\infty T/\delta \approx 5$, where $U_\infty T$ defines a turbulence length scale [Tennekes and Lumley, 1972]. Combining data from the Polomet and Wabash rivers, Jackson found that on average $U_\infty T/\delta \approx 7.6$, which is closer to the slope we calculated.

Surface current retrievals validation

The surface flow estimates from the different algorithms correlate well as depicted in Figure 2a where the run mean flow magnitudes are compared. Strongest correlation exists between the spectral advective surface method and the DPIV, with $r^2=0.96$. The correlation is weaker between the OF estimates and the SAS estimates, but none the less high, with $r^2=0.87$. The correlation coefficient for the DPIV and the OF magnitudes is of 0.84. For mean flows of under 0.8 m/s the OF and DPIV magnitudes are almost on the 1:1 line, however, for stronger flows the DPIV gives surface current magnitudes up to 1 m/s higher than the OF.

Comparing the magnitudes of the velocities derived from the Skin temperature with the 3 different methods to those measured by the ADV, we see good agreement between the measured and the IR derived velocities (c.f. Figure 2b). The correlation coefficients between the ADV measured velocity magnitudes are high: $r^2 = 0.80$ for the DPIV, $r^2 = 0.79$ for the OF, and $r^2 = 0.87$ for the SAS flow magnitudes. Taking the top good bin of the ADCP, which is at around ~ 0.4 m depth, the surface derived velocity are again compared to in situ giving $r^2 = 0.88$, $r^2 = 0.82$, and $r^2 = 0.92$ for DPIV, OF and SAS estimates respectively. The ADCP current measurements at the height of the ADV correlate with the ADV measurement at $r^2 = 0.88$.

Correlation coefficients do not provide sufficient information to conclude on how imagery derived flows compare to measured subsurface flows as it only provides an insight on how closely they are linearly related, but says nothing about how they compare in actual magnitude. The scatter plots as well as the time series of the ADV flow superimposed with the mean estimates of the 3 imagery algorithms (c.f. Figure 2c), clearly show that not only are they well correlated, but they are also of comparable magnitude.

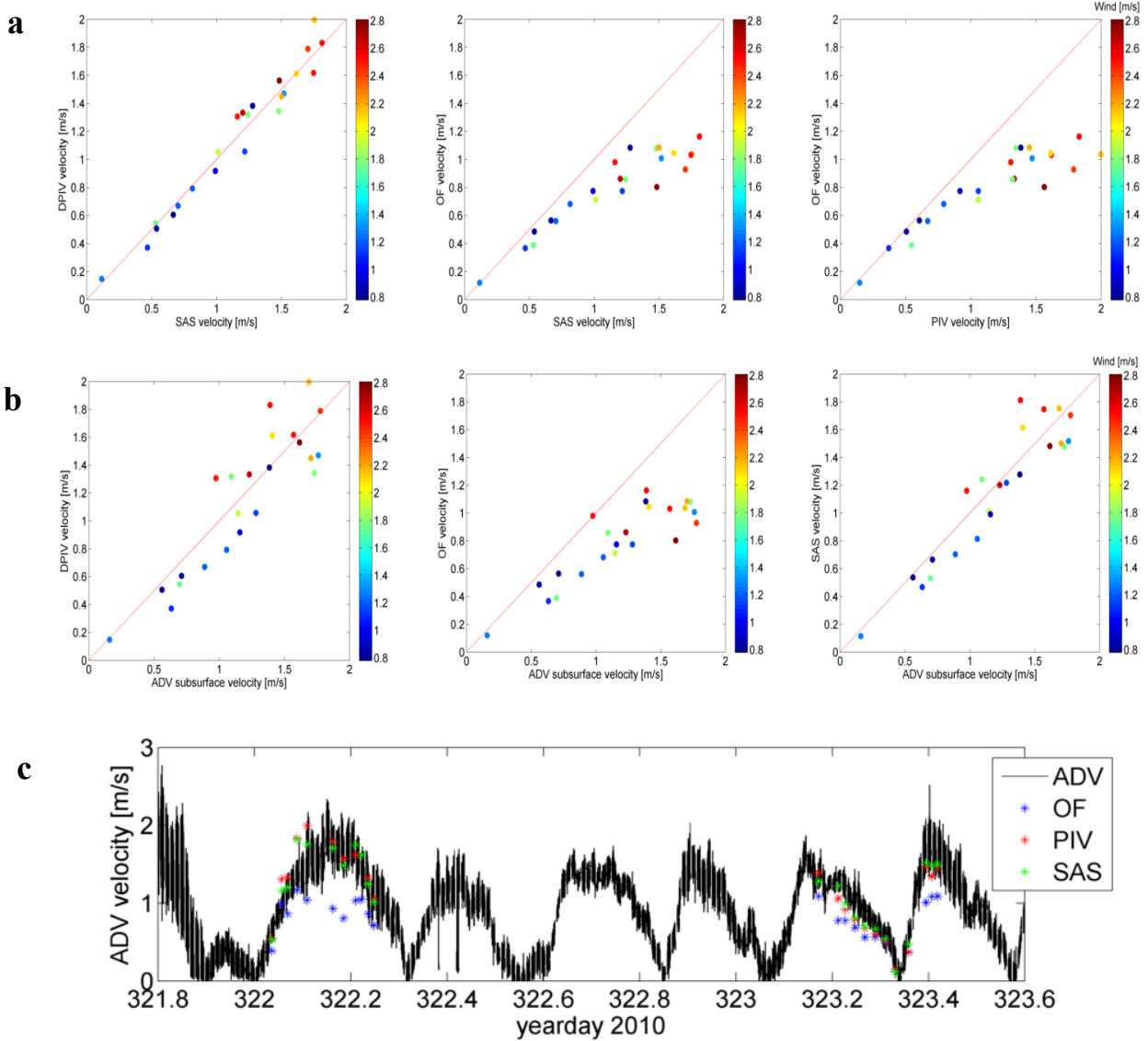


Figure 2 - (a) from left to right: scatter plots of the run mean flow magnitudes derived from the SAS method against those of the DPIV and those of the OF algorithm, and DPIV against OF flow magnitudes. In red the 1:1 line. **(b)** scatter plots of the run mean flow magnitude of the measured and imagery derived flow magnitudes. From left to right: ADV vs. DPIV, ADV vs. OF and ADV vs. SAS. In red the 1:1 line. **(c)** Time series of the flow magnitude measured by the ADV. The colored stars represent the run mean flow magnitudes obtained by the 3 methods: DPIV, OF and SAS.

TKE Dissipation

The turbulent kinetic energy (TKE) dissipation rate ϵ can be estimated by fitting the inertial subrange of wavenumber spectra ($\Phi(k)$) with a $k^{-5/3}$ slope following the Kolmogorov turbulence cascades which dictates that:

$$\Phi(k) = \alpha \epsilon^{2/3} k^{-5/3}$$

Where k denotes the wavenumber and α is a constant. Wavenumber spectra can be computed directly from the IR derived velocity fields or Aquadopp profiles. However, for time series measurement of velocities such as collected by ADVs, it is necessary to make a further assumption in order to derive TKE dissipation rates. Assuming that the frozen Taylor hypothesis is valid, i.e. that turbulent eddies remain unchanged while being advected by the mean flow, one can convert frequency spectra $S(f)$ into wavenumber spectra as follows:

$$\Phi(k) = S(f) \cdot \frac{\langle v \rangle}{2\pi}, \text{ with } k = 2\pi f / \langle v \rangle$$

where f is the frequency and $\langle v \rangle$ the mean velocity.

Surface derived TKE dissipation rates match the subsurface dissipations well (c.f. Figure 3). However, the correlation is worse when the Taylor Hypothesis had to be employed for the subsurface, giving significantly lower correlations ($r^2=0.35$) between the DPIV and ADV derived dissipation rates. The correlation is high ($r^2=0.8$) when the dissipation is calculated directly from wavenumber spectra, even when compared to the bottom instruments. The strong correlation throughout the water column is to be expected from the low shear and stratification.

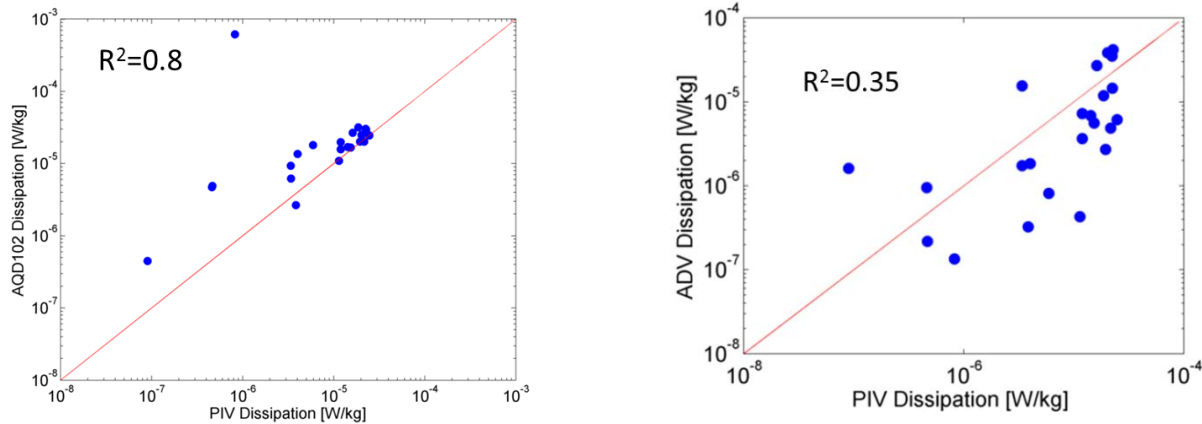


Figure 1 – DPIV derived TKE dissipation rates versus (left) that from the Bottom Aquadopp at 1.83 m above the river bed and (right) that from the ADV at 3.35 m above the river bed

IMPACT/APPLICATIONS

Although in this field campaign the IR remote sensing was performed from a ship, the analysis and results obtained in this study should be easily adaptable to imagery taken from other platforms such as aircrafts, manned and unmanned, as well as fixed platforms. This study reinforces the idea that IR remote sensing is an excellent surveying tool for estuarine environments and encourages continued research in the field. The strong linear relation between depth and surface integral length scales derived from the temperature fields may provide a useful method to estimate bathymetry, especially when no waves are present.

The good agreement between the IR derived and sub-surface TKE dissipation estimates reinforces the adequacy of IR remote sensing for studies of estuarine and riverine turbulence. Previous studies have already shown how IR derived dissipation rates reflects in situ measured dissipation well [e.g. Chickadel et al. 2011]. Unlike us, they made use of the Taylor hypothesis even for the imagery estimates, choosing to compute dissipation at a single location. Our results strongly suggest that not having to assume the validity of the Taylor hypothesis gives significantly better results.

REFERENCES

Brumley, B. H., and G. H. Jirka (1988), Air-water transfer of slightly soluble gases: Turbulence, interfacial processes and conceptual models, *PhysicoChemical Hydrodynamics*, 10(3), 295-319.

Chickadel, C. C., S. A. Talke, A. R. Horner-Devine, and A. T. Jessup (2011). Infrared-based measurements of velocity, turbulent kinetic energy, and dissipation at the water surface in a tidal river. *Geoscience and Remote Sensing Letters*, GRSL-00530-2010.R1.

Dugan, J.P. and C.C. Piotrowski (2012), Measuring currents in a coastal inlet by advection of turbulent eddies in airborne optical imagery, *Journal of Geophysical Research*, 117, C03020, 15 PP., doi:10.1029/2011JC007600.

Jackson, R.G. (1976). Sedimentological and fluid-dynamic implications of the turbulent bursting phenomenon in geophysical flows. *J. Fluid Mech.*, vol. 77, 531-560.

Korchoka Y. M. (1968). Investigation of the dune movement of sediments on the Polomet' River. *Sov. Hydrol.* 541-559.

McKenna, S. P., and W. R. McGillis (2004), The role of free-surface turbulence and surfactants in air-water gas transfer, *International Journal of Heat and Mass Transfer*, 47, 539-553.

Rao, K. N., R. Narasimha, and M.A. Badri Narayanan (1971). The ‘bursting’ phenomenon in a turbulent boundary layer. *J. Fluid Mech.*, 48, 339-352.

Tennekes, H., and J.L. Lumley (1972). A First Course in Turbulence. MIT Press, Cambridge, Mass.